ORIGINAL ARTICLE

Modification of Silica surface by Titanium sol synthesis and characterization

Tayseir Mohammad Abd Ellateif [1,2]; Saikat Maitra [3]*

[1]*Chemical Engineering Department, University Technology PETRONAS, Tronoh, Perak, Malaysia*
[2]*Gas Processing Center, College of Engineering, Qatar University, Doha, Qatar*
[3]*Government College of Engineering and Ceramic Technology, Kolkata, India*

Abstract
Hydrophobic silica titanium nanoparticles (STNPs) were successfully synthesized by the sol-gel process using liquid modification. Fourier transform infrared (FTIR) and X-ray fluorescence (XRF) studies were demonstrated the attachment of titanium on the silica surface. Titanium content enhanced the agglomeration of particles as shown in topography results. The N_2 adsorption-desorption followed Type (V) isotherm indicating the meso-porous nature of the synthesized pure silica. However, STNPs followed type (II) isotherms representing the presence of the large pores. The presence of titanium reduced the surface area of silica nanoparticles with an increase in pore volume and size. Amorphous nature of the synthesized STNPs was observed using X-ray diffraction (XRD). The synthesized pure silica and STNPs exhibited considerable thermal stability up to 800 ° C. The thermo-gravimetric analysis along with the hydrophobicity test confirmed the hydrophobic nature of synthesized silica titanium nanoparticles.

Keywords: *Hydrophobicity, Mesoporosity, Silica nanoparticles, Sol-gel, Surface modification, Titanium.*

INTRODUCTION

Silica nanoparticles have become one of the most attractive materials in recent time for its wide range of applications owing to some of their excellent properties, e.g., high specific surface area, light translucency, ease in manipulation of fabrication and last but not least, low cost [1, 2]. Silica nanoparticles were synthesized in different forms with a silica as thin as a single nanometer (nanotubes) [3], nanospheres [3], ultrathin films [4] and meso-porous silica [5]. Silica can be prepared with numerous topological forms with high surface area, porosity and different thermal, chemical and mechanical stability [6], making them suitable for applications in photonics, drug-delivery [7-9] microelectronics [10], catalysis [11] and different biotechnological applications [7, 8]. Furthermore, silica nanoparticles have been used as solid materials for environmental adsorption or separation applications [12-14]. Silica surfaces, thin films, and silica nanostructures in

* Corresponding Author Email: *tayseir07@yahoo.com*

general, are known to possess characteristics which are quite unlike of the physical/chemical properties of the bulk [15].

The preparation techniques of silica nanoparticles can be classified into three main categories included the reverse microemulsion, flame synthesis and the widely utilized Stober sol-gel method [16-18]. Both reverse microemulsion and sol-gel methods are based on the hydrolysis and condensation of tetraethyl orthosilicate (TEOS) and tetramethyl orthosilicate (TMOS) under acidic or basic conditions [19]. The synthesized silica nanoparticles using these two methods have spherical shapes with smooth surfaces covered by hydroxyl groups [17, 20]. The surfactant molecules dissolve in organic solvents forming spherical micelles in the presence of water in the reverse micro-emulsion method. Polar head groups containing water then organize themselves to form micro-cavities called reverse micelles.

During the synthesis of silica nanoparticles, the nanoparticles can be grown inside the micro-cavities by careful control of silicon alkoxides and the added catalyst into the medium containing reverse micelles. The high cost of the final products and difficulties in the removal of surfactants are considered as major disadvantages of the reverse micro-emulsion method. However, the method was successfully used for the use of nanoparticles as coating materials with a series of functional groups for different applications [21, 22]. Due to the high surface energy and abundant hydroxyl groups (silanol- Si-OH) on the silica surface, these nano-particles tend to agglomerate developing a weak affinity with the polymer matrix and therefore render them hydrophilic materials. Although many advances have been achieved in the applications of silica nanoparticles, surface modification is commonly required in order to achieve better performance. The most convenient way to develop a chemically modified surface is fixing the chemical compound, for instance, alcohol [23, 24], surfactant, and silane or titanate coupling agent on the surface of silica [25-27]. Titania–silica mixed oxides are of significant importance in photocatalytic applications due to their high photocatalytic activity. The interaction between TiO_2 and SiO_2 results in new structural and physicochemical properties such as quantum-sized crystallinity, high surface area, high adsorption capacity and high acidity [11, 28]. The hydrophilic nature of the synthesized silica hinders their use in many applications. Therefore, this work is focusing in the synthesis and modification of silica nanoparticles via the sol gel process to convert silica to hydrophobic materials using liquid modification. Titanium sol was selected as the modifier with different content. The effect of titanium content in the synthesized hydrophobic silica nanoparticles texture and properties is the aim of the work.

EXPERIMENTAL

Materials

Tetraethyl orthosilicate (TEOS 98% purity) and titanium (IV) isopropoxide (98% purity) purchased from ACROS ORGANICS. Ethanol (95%) from HmbG chemicals and ammonia (25% purity) purchased from R & M chemicals. All the chemicals were used without further purification.
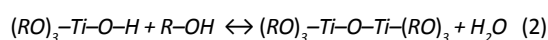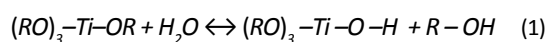
Synthesis of silica sol

(0.5 M) TEOS was used as the starting material

and ammonia (0.5 M) was used as base catalyst, then distilled water was added. The molar ration between TEOS, NH_3 and H_2O was 0.5, 0.5 and 10 respectively. Due to the low solubility of TEOS in water, ethanol was added as dispersant. The prepared mixtures were stirred at 100 rpm at room temperature (25°C) for one hour to produce silica sol.

Synthesis of Titanium sol

Titanium sol was synthesized following the method suggested by López *et al.* [29] by mixing titanium tetrapropoxide (30 ml) with 100 ml of ethanol. The mixture was stirred for 30 minutes followed by sonication (30 minutes). Then 24 ml of distilled water was added at the rate of 1 ml /min with continuous stirring [30]. The mixture was kept in the oven at 95°C for 24 h to produce titanium oxide as shown in equation 1 and 2.

$$(RO)_3-Ti-OR + H_2O \leftrightarrow (RO)_3-Ti-O-H + R-OH \quad (1)$$

$$(RO)_3-Ti-O-H + R-OH \leftrightarrow (RO)_3-Ti-O-Ti-(RO)_3 + H_2O \quad (2)$$

Silica Surface Modification

The synthesized titanium sol was added to silica sol with different percentages of volume: 1, 3 and 5, to produce the modified silica nanoparticles as shown in equation 3. The silica surface modification and the predicted structure are shown in Fig. 1 and Fig. 2 (a, b) using Chemsketch software [31].

$$Si-OH + TiO_2 \rightarrow \equiv Si-O-Ti\equiv + H_2O \quad (3)$$
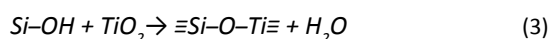
Surface characterization

Different techniques were used to investigate the characteristic of the synthesized pure and modified silica nanoparticles. The composition of the synthesized pure silica and silica titanium nanoparticles (STNPs) was confirmed using X-ray fluorescence XRF (4kW S4 PIONEER) and Fourier transforms infrared FTIR (Shimadzu FTIR-8400S). The effect of titanium content on the morphology and particle distribution were studied using field emission scanning electron microscopy FESEM (Zeiss, SUPRA 55VP) and Transmission electron microscopy TEM (Zeiss, Libra 200) respectively. X-ray diffraction pattern XRD (Bruker A & S D8) and thermo-gravimetric analysis TGA (Perkin-Elmer, Pyris V-3.81) were used to study the crystallinity structure and thermal stability. The surface area, pore volume and pore size were measured using liquid N_2 at 77K (Micromeritics ASAP 2000).

RESULT AND DISCUSSION

Chemical composition of the synthesized silica XRF

X-ray fluorescence (XRF) is utilized for the determination of the chemical compositions of the synthesized pure and modified silica nanoparticles and to confirm that the titanium oxides were anchored to the silica surface using liquid modification. The data given in Table 1 shows the composition of pure silica and STNPs. Silica and oxygen are present in major quantities while titanium intensity is present in traces amount as shown in Table 1. The results have exhibited that the intensity of the titanium increases with increasing percentage from 1% to 3% and then to 5%.

Structure of the synthesized silica FTIR

FTIR spectra of the synthesized pure silica nanoparticles display the surface Si-H stretching vibration at 800 cm^{-1}. The adsorption peaks present at 900 cm^{-1} and 1631 cm^{-1} indicate the presence of Si-OH and C-H respectively. The bands at 1090-1230 cm^{-1} confirm the presence of silicon oxide (Si-O-Si), another band appears at 3250-3700 cm^{-1} indicating that there is moisture at the surface of silica nanoparticles (Fig. 3a). FTIR spectra for silica nanoparticles modified with different percentage of titanium are presented in Fig. 3.

In comparison between the three spectra, an adsorption peak of Ti- O, Si- O and Ti- O -Si is
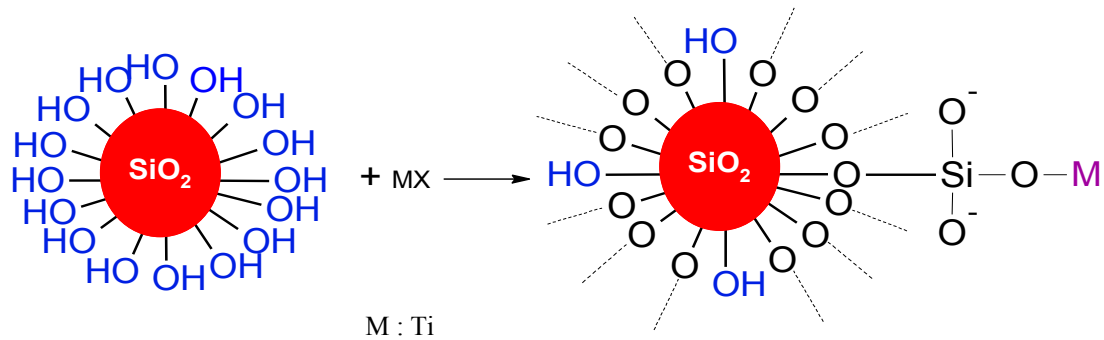

M : Ti

Fig. 1: Silica surface modification.
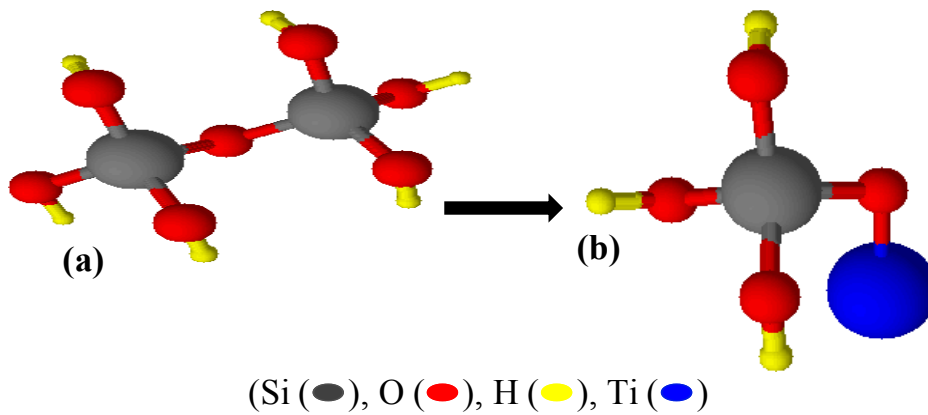

(Si (⚫), O (🔴), H (🟡), Ti (🔵))

Fig. 2: Predicted structure of (a) Pure Silica and (b) STNPs.

Table 1: XRF of the synthesized pure silica and STNPs.

Sample	Modifier %	Intensity (KCps)		
		Si	O	Ti
Pure silica	-	45.66	53	0
Silica titanium	1%	46.7	53	0.14
	3%	46.3	53	0.39
	5%	46.3	53	0.53

observed at 800–900, 1000–1200, and 950 cm^{-1}, respectively [32]. The gradual and monotonic increase in the absorbance at 950 cm^{-1} was accompanied by a decrease in intensity of the resonance at 971 cm^{-1} with the percentage of titanium clearly indicating the replacement of Si-OH with Si-O-Ti (Fig. 3b, 3c, and 3d). FTIR analysis of the silica modified with different percentage of titanium shows a sharpening of the Si–O–Si and Si–O–Ti vibration bands that are accompanied by a disappearance of the silanol band from the particles. These confirm the results established using XRF for pure silica and modified silica nanoparticles with different percentages of titanium.

Hydrophobicity of the synthesized silica

The presence of the OH group at the silica surface is responsible of the silica hydrophilic nature. Drying of silica involves the esterification reaction between the OH groups at the surface of silica and ethanol. This phenomenon results in the formation of alkoxysilane groups that are responsible for the hydrophilic property of the silica [33, 34]. The synthesized pure and modified silica nanoparticles were tested for their hydrophobicity by exposing them to atmospheric moisture at 25°C and measuring the water adsorption by weight

gain [35]. Fig. 4 showed the results of pure silica compared to silica modified with titanium. The synthesized pure silica depicted a weight gain of 8% over a period of 60 days. On the other hand the modified silica showed a weight gain of 3%, 2% and 1% over the entire period depending on the titanium percentage. The low weight gain of STNPs compared to the pure silica nanoparticles illustrated the hydrophobicity nature of the modified silica nanoparticles.

Morphology of the synthesized silica FESEM

FESEM results for pure silica and silica modified with (1, 3, and 5%) titanium with magnification 2000 KX are shown in Fig. 5. The FESEM of pure silica showed that silica nanoparticles have small size and low packing density. The particles are well dispersed and possess a smooth surface with uniform distribution of particles (Fig. 5a). The morphology of silica modified with 1% titanium is dense compared to pure silica (Fig. 5b). While silica modified with 3% titanium has uniform distribution of spherical particles with particle agglomeration (Fig. 5c).

However, for silica modified with 5% titanium there is significant agglomeration of the particles along the grain boundary resulting in the formation of secondary particles (Fig. 5d).
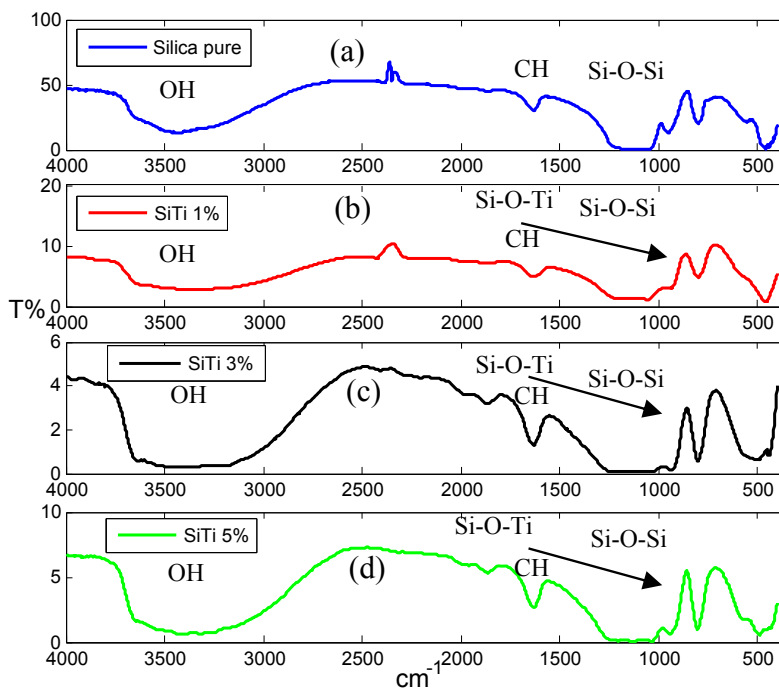

Fig. 3: FTIR of (a) unmodified silica (b) STNPs 1% (c) STNPs 3% (d) STNPs 5%.
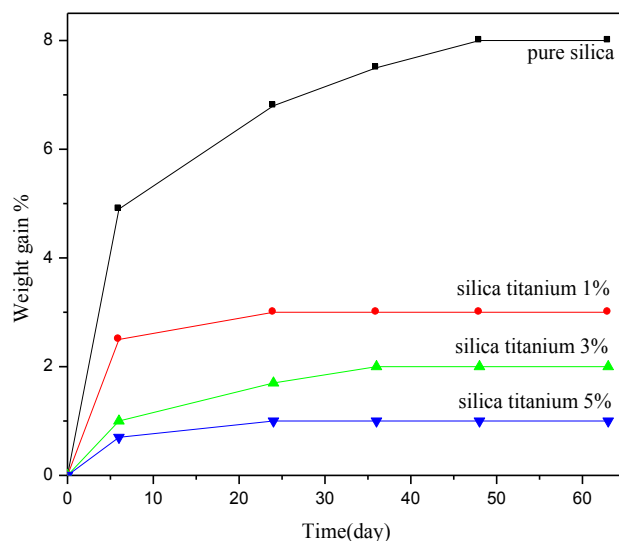
Fig. 4: Hydrophobicity of the synthesized pure silica and STNPs.

Particle distribution of the synthesized silica TEM

The particles distribution of the synthesized STNPs were observed using TEM. For pure silica nanoparticles, TEM micrographs illustrated spherical particles with particle sizes ranging from 27 nm to 35 nm as shown in Fig. 5e. Silica titanium 1% demonstrated silica nanoparticles with sizes from 31 nm to 33 nm agglomerate around spherical titanium nanoparticles with particle size of 54 nm to 73 nm (Fig. 5f). However, silica titanium 3% (Fig. 5g) showed silica nanoparticles with sizes ranging from 36 nm to 37 nm agglomerate around the titanium nanoparticles, the sizes of which range from 75 nm to 113 nm. In contrast, silica modified with 5% titanium (Fig. 5h) illustrated more agglomeration of small silica nanoparticles (27 nm) around titanium particles (63 nm to 81 nm). Obviously, silica titanium TEM micrograph showed agglomeration which affected the morphology of the STNPs. Additionally particles agglomerations have considerable effect on the morphology and surface area of the synthesized STNPs.

Surface area of the synthesized silica BET

To investigate the effect of titanium in the surface area of the synthesized STNPs, BET equation was used for measuring the surface area of the pure and modified silica nanoparticles. The surface area and pore size analyzer results showed the surface area of pure silica nanoparticles was 303.69 m^2/g with pore size 4.36 nm (Table 2). The surface area of STNPs illustrates a high reduction in surface area of silica. This result can be related to the fact that titanium enhanced the agglomeration and aggregation of silica nanoparticles as discussed in FESEM and TEM results. Moreover, increase in the pores size from 4.36 to 25.2 nm decreases the surface area of STNPs. BET surface area clearly depends on the percentage of titanium. The N_2 adsorption-desorption isotherms of pure silica (Fig. 6a) showed type (V) indicating the meso-porosity (pore size 2-50 nm) [20] of the synthesized pure silica which is in good agreement of the pore size calculated using BJH equation (Table 2). Nevertheless, N_2 adsorption-desorption isotherms of STNPs followed type (II) isotherm indicating the presence of large pores. The reduction in the pore volume (Fig. 6b) and increase in the pore size with the increase in titanium content is responsible for the surface area drop.

Crystallite of the synthesized silica XRD

X-ray diffraction (XRD) was used to determine the crystalline structure of the silica particles. Silica nanoparticles are amorphous materials according to XRD with peaks 2θ = 25° as shown in Fig. 7. The XRD results showed that the Si-O-Ti particles are amorphous and 2θ is around 15° (Fig. 7). No peaks for the crystalline silica phase were observed. All silica nanoparticles modified with titanium, are amorphous regardless of the amount of titanium added to the silica and 2θ is around 15° due to the presence of titanium in the samples. The result is similar to silica titanium XRD observed from the literature [36].
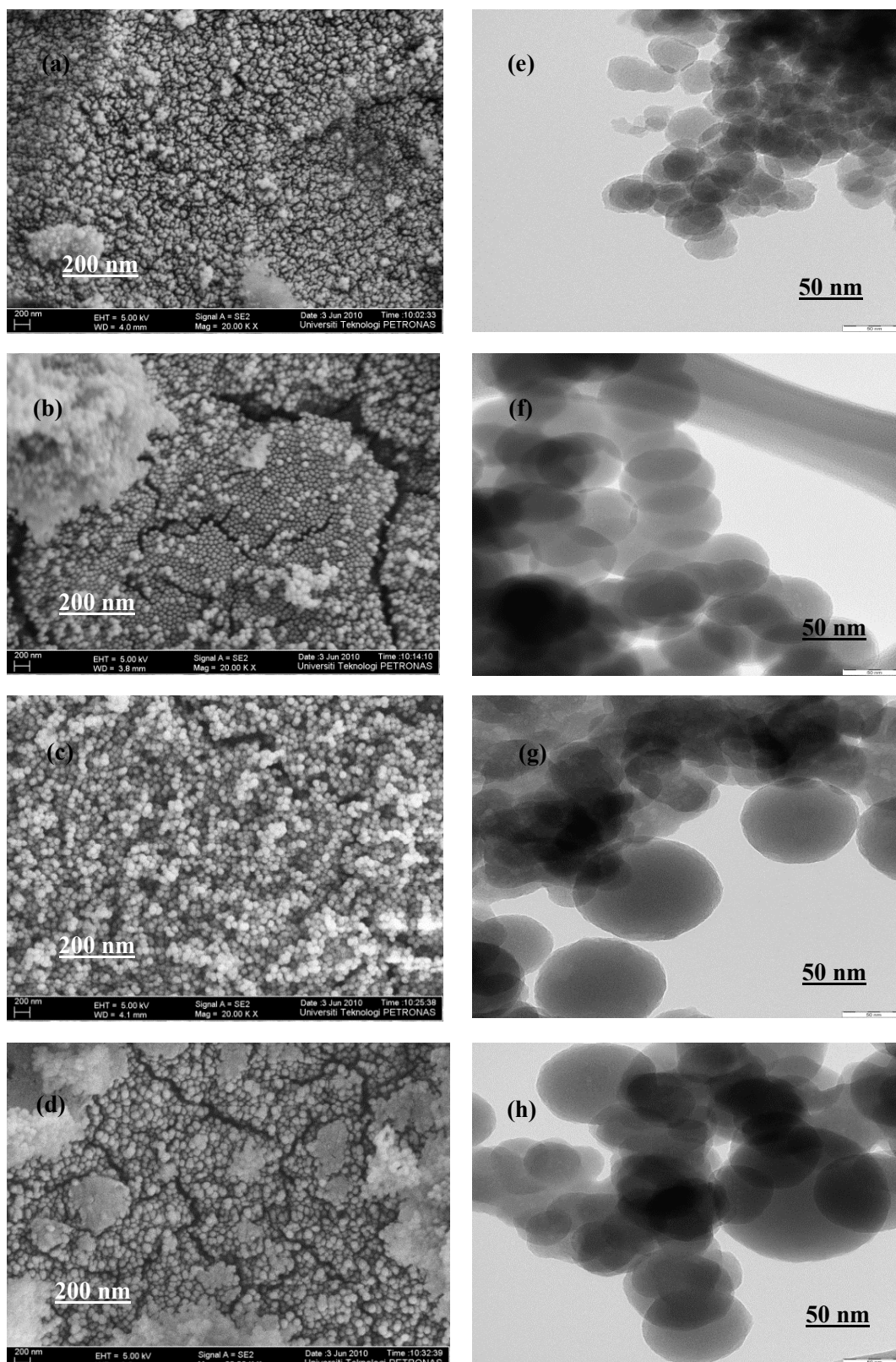
Fig. 5: FESEM of the (a) unmodified silica nanoparticles (b) STNPs 1% (c) STNPs 3% (d) STNPs 5% and TEM of the (e) unmodified silica nanoparticles (f) STNPs 1% (g) STNPs 3% (h) STNPs 5%.
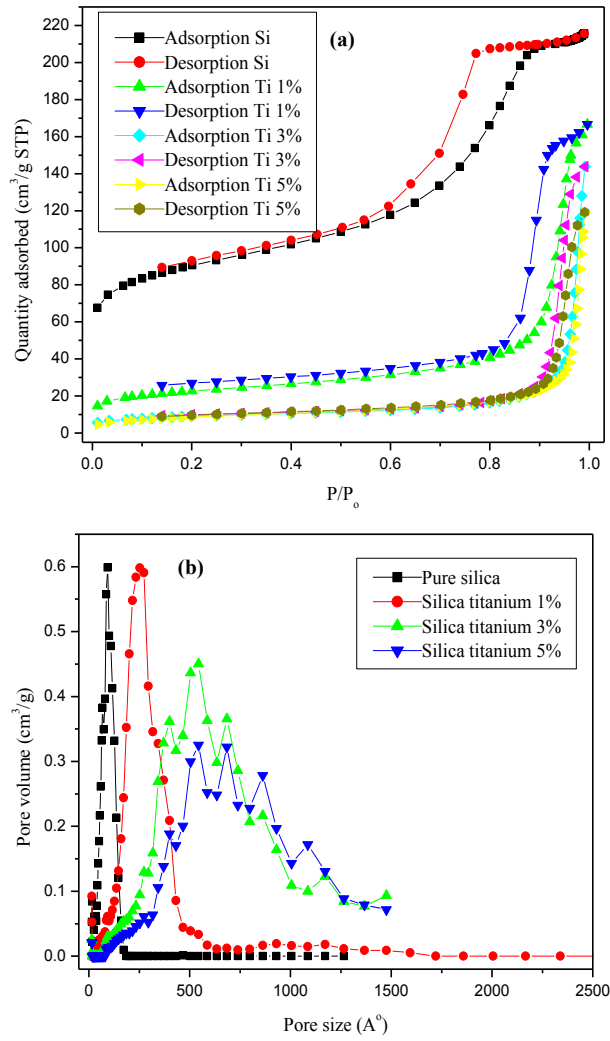
Fig. 6: The synthesized silica and STNPs (a) N$_2$ adsorption-desorption isotherms (b) pore size and pore volume distribution.
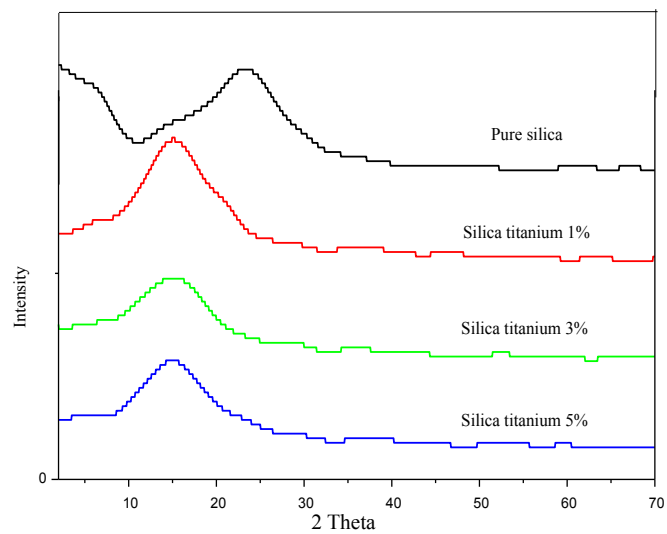

Fig. 7: XRD of the synthesized pure silica and STNPs.

Thermal stability of the synthesized silica TGA

TGA shows the thermal decomposition behaviors of pure silica nanoparticles and silica modified with titanium. The thermal stability is a significant factor that determines the applicability of the materials for high temperature applications. Moreover, the proportions of physically adsorbed water and hydroxyl groups of nanoparticles are evaluated quantitatively by TGA. For pure silica nanoparticles the first 9% of weight is lost between 0 and 100°C, due to the loss of adsorbed water and moisture in the sample. The second 14% of weight is lost between 100°C and 400°C, due to the loss of strongly bonded (hydrogen bonded) water molecules. The final 16% is lost between 400°C and 800°C, because of the condensation of silanol groups (Si-OH) to siloxane bonds (Si-O-Si) with the removal of water. The

Thermo-gravimetric analysis has depicted the high thermal stability of synthesized silica up to 800°C [37-40]. Modified silica nanoparticles showed higher thermal stability compared to pure silica. Silica titanium 1% demonstrated lower thermal stability as shown in Fig. 8. While silica modified with 3% titanium exhibited its best thermal stability at a temperature range of 100-400°C. On the other hand silica titanium 5% showed the highest thermal stability at temperatures between 100-400°C and similar thermal stability with silica titanium 3% at temperatures ranging from 400-800°C, this is due to the distribution and agglomeration of the titanium particles at the surface of the silica as shown in TEM result. The low weight losses of STNPs compared to pure silica confirms the hydrophobicity of the synthesized STNPs.

Table 2: Surface area of the synthesized pure silica and STNPs.

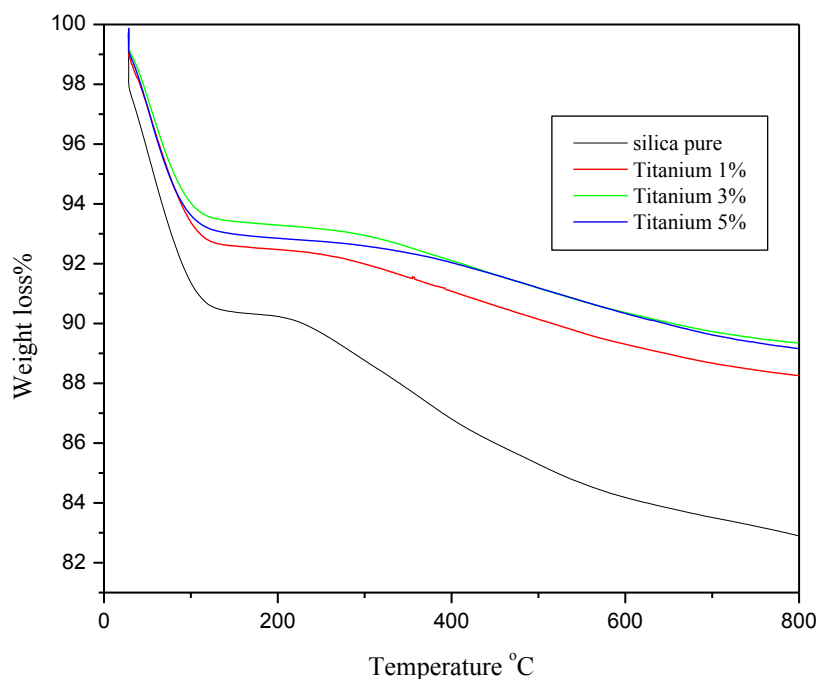| Sample	Modifier %	BET m^2/g	Pore size nm	Pore volume cm^3/g
Pure silica nanoparticles	-	303.69	4.36	0.33
Silica titanium	1%	77.93	12.70	0.24
	3%	31.42	19.28	0.19
	5%	31.03	25.20	0.14

Fig. 8: Thermal stability of the synthesized pure silica and STNPs (TGA).

CONCLUSION

Hydrophobic silica titanium nanoparticles (STNPs) were synthesized using the sol gel process and liquid modification. The influence of titanium content on the physical characteristics of silica was investigated. FTIR and XRF have confirmed the presence of titanium at the surface of the silica. The hydrophobicity test illustrated weight gain of 8% for the pure silica and 3%, 2% and 1% for the STNPs (1, 3 and 5%) respectively over the entire period. The FESEM and TEM micrograph showed that the introduction of titanium enhanced the agglomeration and aggregation of particles. Due to agglomeration of particles there is a decrease in surface area and an increase in pore size of silica titanium particles. The synthesized silica titanium nanoparticles are amorphous materials with 2θ at 15°. The thermal analysis depicted high thermal stability up to a temperature 800 ˚C and lower weight loss for the silica titanium nanoparticles compared to pure silica. The agreement between the hydrophobicity test and TGA results confirm the hydrophobicity of the synthesized silica titanium nanoparticles.

CONFLICT OF INTEREST

The authors declare that there is no conflict of interests regarding the publication of this manuscript.

REFERENCES

[1] Bao B., Li F., Li H., Chen L., Ye C., Zhou J., Wang J., Song Y., Jiang L., (2013), pH-responsive dual fluorescent core-shell microspheres fabricated via a one-step emulsion polymerization. *J. Mater. Chem. C.* 1: 3802-3807.

[2] Li M., Lam J. W. Y., Mahtab F., Chen S., Zhang W., Hong Y., Xiong J., Zheng Q., Tang B. Z., (2013), Biotin-decorated fluorescent silica nanoparticles with aggregation-induced emission characteristics: fabrication, cytotoxicity and biological applications. *J. Mater. Chem. B.* 1: 676-684.

[3] Wang L., Tomura S., Ohashi F., Maeda M., Suzuki M., Inukai K., (2001), Synthesis of single silica nanotubes in the presence of citric acid. *J. Mater. Chem.* 11: 1465-1468.

[4] Muller D. A., Sorsch T., Moccio S., Baumann F. H., Evans-Lutterodt K., Timp G., (1999), The electronic structure at the atomic scale of ultrathin gate oxides. *Nature*. 399: 758-761.

[5] Monnier A., Schüth F., Huo Q., Kumar D., Margolese D., Maxwell R. S., Stucky G. D., Krishnamurty M., Petroff P., Firouzi A., Janicke M., Chmelka B. F., (1993), Cooperative formation of inorganic-organic interfaces in the synthesis of silicate mesostructures. *Science*. 261: 1299-1303.

[6] Barandeh F., Nguyen P.-L., Kumar R., Iacobucci G. J., Kuznicki M. L., Kosterman A., Bergey E. J., Prasad P. N., Gunawardena S., (2012), Organically modified silica nanoparticles are biocompatible and can be targeted to neurons in vivo. *PLoS ONE*. 7: 1-15.

[7] Hwang T., Lee H. Y., Kim H., Kim G. T., (2010), Two layered silica protective film made by a spray-and-dip coating method on 304 stainless steel. *J. Sol-Gel Sci. Technol*. 2010: 1-6.

[8] Oh Y. K., Hong L. Y., Asthana Y., Kim D. P., (2006), Synthesis of super-hydrophilic mesoporous silica via a sulfonation route. *JIEC*. 12: 911-917.

[9] Maggini L., Cabrera I., Ruiz-Carretero A., Prasetyanto E. A., Robinet E., Cola L. De, (2016), Breakable mesoporous silica nanoparticles for targeted drug delivery. *Nanoscale*. 8: 7240-7247.

[10] Giesche H., (1994), Synthesis of monodispersed silica powders I. Particle properties and reaction kinetics. *J. Eur. Ceram. Soc.* 14: 189-204.

[11] Yang S., Sun C., Li X., Gong Z., Quan X., (2010), Enhanced photocatalytic activity for titanium dioxide by co-modifying with silica and fluorine. *J. Hazard. Mater*. 175: 258-266.

[12] Wang N., Zhou L., Guo J., Ye Q., Lin J.-M., Yuan J., (2014), Adsorption of environmental pollutants using magnetic hybrid nanoparticles modified with β-cyclodextrin. *Appl. Surf. Sci.* 305: 267-273.

[13] Liu J., Ma S., Zang L., (2013), Preparation and characterization of ammonium-functionalized silica nanoparticle as a new adsorbent to remove methyl orange from aqueous solution. *Appl. Surf. Sci.* 265: 393-398.

[14] Vakili D., Attarnejad M. A., Massoodian S. K., Akbarnejad M. M., (2005), Synthesis of hydrophobic silicalite adsorbent from domestic resources: The effect of alkalinity on the crystal size and morphology. *IJCCE*. 24: 9-14.

[15] Flikkema E., Bromley S. T., (2003), A new interatomic potential for nanoscale silica. *Chem. Phys. Lett*. 378: 622-629.

[16] Lin Y. S., (2001), Microporous and dense inorganic membrane :current status and prospective. *Sep. Purif. Technol*. 25: 39-55.

[17] Zou H. W., Shen S., (2008), Polymer/silica nanocomposites: Preparation, characterization, properties, and applications. *Chem. Rev*. 108: 3893-3957.

[18] Hench L. L. W., (1990), The sol-gel process. *Chem. Rev*. 90: 33-72.

[19] Brinker C. J., (1988), Hydrolysis and condensation of silicates: Effects on structure. *J. Non-Cryst. Solids*. 100: 31-50.

[20] Xu S., Hartvickson S., Zhao J., (2011), Increasing surface area of silica nanoparticles with a rough surface. *ACS Applied Materials & Interfaces*. 3: 1865-1872.

[21] Liu S., Han M. Y., (2010), Silica-coated metal nanoparticles. *Chem. Asian. J.* 5: 36-45.

[22] Bagwe R. P., Hilliard L. R., Tan W., (2006), Surface modification of silica nanoparticles to reduce aggregation and nonspecific binding. *Langmuir*. 22: 4357-4362.

[23] Jesionowski T., Krysztafkiewicz A., (1999), Properties of highly dispersed silicas precipitated in an organic medium. *J. Dispersion Sci. Technol*. 20: 1609-1623.

[24] An D., Wang Z., Zhao X., Liu Y., Guo Y., Ren S., (2010), A new route to synthesis of surface hydrophobic silica with long-chain alcohols in water phase. *Colloids Surf. A: Physicochemical and Engineering Aspects*. 369: 218-222.

[25] Dékány I., Szántó F., Nagy L. G., (1985), Sorption and immersional wetting on clay minerals having modified surface. I. Surface properties of nonswelling clay mineral organocomplexes. *J. Colloid Interface Sci*. 103: 321-331.

[26] Vrancken K. C., Possemiers K., Van Der Voort P., Vansant E. F., (1995), Surface modification of silica gels with aminoorganosilanes. *Colloids Surf. A: Physicochemical and*

Engineering Aspects. 98: 235-241.

[27] Daniels M. W., Francis L. F., (1998), Silane adsorption behavior, microstructure, and properties of glycidoxypropyltrimethoxysilane-modified colloidal silica coatings. *J. Colloid Interface Sci*. 205: 191-200.

[28] Hüsing N., Launay B., Doshi D., Kickelbick G., (2002), Mesostructured silica–titania mixed oxide thin films. *Chem. Mater*. 14: 2429-2432.

[29] López T. M., Avnir D., Aegerter M. A., (2003), *Emerging fields in sol-gel science and technology*: Springer Netherlands.

[30] Tayade R. J., Kulkarni R. G., Jasra R. V., (2006), Transition metal ion impregnated mesoporous TiO_2 for photocatalytic degradation of organic contaminants in water. *Ind. Eng. Chem. Res*. 45: 5231-5238.

[31] Abd Ellateif T. M., Maitra S., (2017), Some studies on the surface modification of sol-gel derived hydrophilic Silica nanoparticles. *Int. J. Nano Dimens*. 8: 97-106.

[32] Park O. K., Kang Y. S., (2005), Preparation and characterization of silica-coated TiO_2 nanoparticle. *Colloids Surf. A: Physicochemical and Engineering Aspects*. 257: 261-265.

[33] Rao A. V., Wagh P. B., (1998), Preparation and characterization of hydrophobic silica aerogels. *Mater. chem. phys*. 53: 13-18.

[34] Wagh P. B., Rao A. V., Haranath D., (1998), Influence of molar ratios of precursor, solvent and water on physical properties of citric acid catalyzed TEOS silica aerogels. *Mater. chem. phys*. 53: 41-47.

[35] Reynolds J., Coronado G., Hrubesh L. W. P. R., (2001), Hydrophobic aerogels for oil-spill clean up-synthesis and characterization. *J. Non-Cryst. Solids*. 292: 127-137.

[36] Lee M., Lee G., Park S., Ju C., Lim K., Hong S., (2005), Synthesis of TiO_2/SiO_2 nanoparticles in a water-in-carbon-dioxide microemulsion and their photocatalytic activity. *Res. Chem. Intermed*. 31: 379-389.

[37] Chiang C. L., Chang R. C., Chiu Y. C., (2007), Thermal stability and degradation kinetics of novel organic/inorganic epoxy hybrid containing nitrogen/silicon/phosphorus by sol-gel method. *Thermochim. Acta*. 453: 97-104.

[38] Ying-Ling Liu W., Hsu K-Y., Ho W-H., (2004), Thermal stability of epoxy-silica hybrid materials by thermogravimetric analysis. *Thermochim. Acta*. 412: 139–147.

[39] Fan X., Lin L., and Messersmith P. B., (2006), Surface-initiated polymerization from TiO_2 nanoparticle surfaces through a biomimetic initiator: A new route toward polymer-matrix nanocomposites. *Compos. Sci. Technol*. 66: 1198-1204.

[40] Zawrah M., El-Kheshen F., Abd-Elaal A., (2009), Facile and economic synthesis of silica nanoparticles. *J. Ovonic Res*. 5: 129-133.